

Chemical Vapor Deposition of Copper from (hfac)CuL (L = VTMS and 2-Butyne) in the Presence of Water, Methanol, and Dimethyl Ether

A. Jain,[†] T. T. Kodas,^{*,†} T. S. Corbitt,[‡] and M. J. Hampden-Smith^{*,‡}

Department of Chemical and Nuclear Engineering and Department of Chemistry,
University of New Mexico, Albuquerque, New Mexico 87131

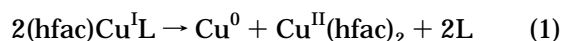
Received November 16, 1995. Revised Manuscript Received February 15, 1996[®]

The CVD of Cu using (hfac)Cu(VTMS) (hfac = hexafluoroacetylacetonate, VTMS = vinyltrimethylsilane) and (hfac)Cu(2-butyne) in the presence of water and other reagents has been studied. The overall CVD reaction involving disproportionation of these copper(I) compounds in the presence of water is similar to the overall reaction in the absence of water. The Cu films deposited at low water vapor flow rate (0.2 sccm) exhibited near bulk resistivities ($\sim 2.0 \mu\Omega$ cm) and dense surface morphologies while the Cu films deposited at higher water vapor flow rate (2.4 sccm) showed significantly higher resistivities ($\sim 12 \mu\Omega$ cm) and porous morphologies. At higher water flow rates the deposition rate and conductivity of the films were reduced as a result of Cu₂O incorporation. The presence of water during CVD is believed to introduce a reaction parallel to the main CVD disproportionation reaction via reaction of water with surface-bound [Cu(hfac)] and results in the incorporation of copper(I) oxide (Cu₂O) in the Cu films. Labeling experiments using H₂O¹⁸ showed that the oxygen incorporated into the films (SIMS) at high water flow rates was derived from reaction with H₂O.¹⁸ The deposition rate enhancements with methanol and dimethyl ether showed similar trends as a function of flow rate but lower overall rate enhancements compared to water. The presence of water is believed to aid the dissociation of the L from the (hfac)CuL by hydrogen bonding with the hfac ligand and/or oxygen donation to the copper(I) center. The incorporation of Cu₂O was completely suppressed by introduction of hfacH vapor along with the precursor and water vapor during CVD of Cu.

Introduction

Chemical vapor deposition (CVD) of copper (Cu) has been extensively studied for applications in IC metalization. This is primarily because several families of well-characterized high-performance precursors are currently available for copper CVD.^{1,2} One family is the copper(I) compounds (hfac)CuL where hfac is 1,1,1,5,5,5-hexafluoroacetylacetonate and L is a neutral ligand. This family of compounds with various substituted neutral ligands such as trimethylphosphine (PMe₃), 1,5-cyclooctadiene (COD), 2-butyne, and vinyltrimethylsilane (VTMS) deposit high-quality films at high rates and low temperatures (150–200 °C).^{3–14}

The nature of the neutral ligand L affects the chemical and physical characteristics of the precursor, the deposition rate, and film morphology. For example, precursors with different neutral ligands exhibit different deposition rates and activation energies^{3–14} for deposition of copper, although they follow a common overall CVD pathway: thermally induced disproportionation as described by eq 1.^{2,12} Also, some of the



precursors such as (hfac)Cu(VTMS) are liquids,^{2,12} while most others are solids at room temperature. Because it is commercially available, is a liquid, and deposits high-quality films, the precursor (hfac)Cu(VTMS) has been studied extensively.^{15,16} Studies of this and other related precursors have led to a fairly clear understanding of the overall CVD pathway and chemistry for (hfac)CuL compounds.^{14,17,18} This understanding has been derived from CVD studies by evaluating deposition

[†] Department of Chemical and Nuclear Engineering.

[‡] Department of Chemistry.

* To whom correspondence should be addressed.

[®] Abstract published in *Advance ACS Abstracts*, April 1, 1996.

(1) Jain, A.; Chi, K.-M.; Shin, H.-K.; Farkas, J.; Kodas, T. T.; Hampden-Smith, M. J. *Semiconduct. Int.* **1993**, June, 128.

(2) Kodas, T. T.; Hampden-Smith, M. J., Eds. *The Chemistry of Metal CVD*; VCH: Weinheim, 1994; Chapters 4 and 5.

(3) Shin, H.-K.; Chi, K.-M.; Hampden-Smith, M. J.; Kodas, T. T.; Paffett, M.; Farr, J. D. *Angew. Chem. Adv. Mater.* **1991**, 3, 246.

(4) Cohen, S. L.; Lieher, M.; Kasi, S. *Appl. Phys. Lett.* **1992**, 60, 50.

(5) Kumar, R.; Maverick, A. W.; Fronczek, F. R.; Lai, G.; Griffin, G. L. 201st ACS meeting (Atlanta, GA), INOR 256 (April 1991).

(6) Jain, A.; Chi, K.-M.; Kodas, T. T.; Hampden-Smith, M. J.; Farr, J. D.; Paffett, M. F. *Chem. Mater.* **1991**, 3, 995.

(7) Jain, A.; Chi, K.-M.; Kodas, T. T.; Hampden-Smith, M. J.; Farr, J. D.; Paffett, M. F. *J. Mater. Res.* **1992**, 7(2), 261.

(8) Jain, A.; Chi, K.-M.; Kodas, T. T.; Hampden-Smith, M. J. *Mater. Res. Soc. Symp. Proc.* **1992**, 260, 113.

(9) Reynold, S. K.; Smart, C. J.; Baran, E. F. *Appl. Phys. Lett.* **1991**, 59, 2332.

(10) Chi, K.-M.; Shin, H. K.; Hampden-Smith, M. J.; Kodas, T. T.; Duessler, E. N. *Inorg. Chem.* **1991**, 30, 4293.

(11) Reynolds, S. K.; Smart, C. J.; Baum, T. H.; Larson, C. E.; Brock, P. J. *Appl. Phys. Lett.* **1991**, 59, 2332.

(12) Hampden-Smith, M. J.; Kodas, T. T. *Polyhedron* **1995**, 14, 699.

(13) Baum, T. H.; Larson, C. E. *Chem. Mater.* **1992**, 4, 365.

(14) Jain, A.; Chi, K. M.; Kodas, T. T.; Hampden-Smith, M. J. *J. Electrochem. Soc.* **1993**, 140, 1434.

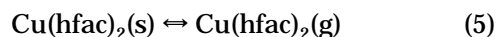
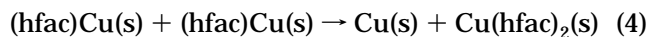
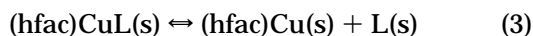
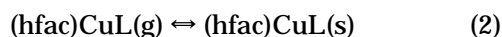
(15) Jeon, N. L.; Nuzzo, R. G. *Langmuir* **1995**, 11, 341.

(16) Chiou, J. C.; Juang, K. C.; Chen, M. C. *J. Electrochem. Soc.* **1995**, 142, 177.

(17) Girolami, G. S.; Jeffries, P. M.; Dubois, L. H. *J. Am. Chem. Soc.* **1993**, 115, 1015.

(18) Cohen, S. L.; Liehr, M.; Kasi, S. *Appl. Phys. Lett.* **1992**, 60, 50.

rates, reaction products, and deposit purity over a wide range of conditions and from ultrahigh vacuum (UHV) studies of the surface chemistry. A number of steps have been proposed based on the available data. The first step involves chemisorption of (hfac)CuL on



the surface (s) with subsequent dissociation of L from the parent molecule, (hfac)CuL, to form the "(hfac)Cu" species (eq 3). This is followed by disproportionation of two surface-bound "(hfac)Cu" species to form Cu(hfac)₂ and Cu metal (eq 4) and finally desorption of the products, Cu(hfac)₂ (eq 5) and L (eq 6) from the surface.¹⁴

In one study, the deposition rate was measured as a function of temperature at constant precursor pressures to obtain activation energies and as a function of pressure at constant temperature to determine the order of the reaction.¹⁴ These data were compared to mathematical expressions for reaction kinetics derived from the proposed CVD pathway and supported dissociation of VTMS from (hfac)Cu(VTMS) as the rate-limiting step.¹⁴ Recent studies of the reaction kinetics of this process have shown that addition of water (H₂O) vapor during CVD of Cu using (hfac)Cu(VTMS) increases deposition rates almost by a factor of 2 while maintaining the film resistivity close to the value for bulk copper.^{19–27} It appears that water participates in the reaction pathway in a beneficial manner.

Although the mechanism of CVD of Cu in the *absence* of water has been studied extensively, there is no clear understanding of the process in the *presence* of water vapor. For example, the reasons for the increase in deposition rate when small quantities of H₂O vapor are introduced during CVD and whether this effect also occurs for other (hfac)CuL compounds are not known. Studies are also needed to identify possible impurity phases as a function of water vapor flow rate and to determine the reasons for their incorporation in the films. This information is necessary to develop strategies for deposition of high-purity copper films in the presence of water vapor to take advantage of the deposition rate enhancement.

(19) Gelatos, A. V.; Marsh, R.; Kottke, M.; Mogab, C. J. *Appl. Phys. Lett.* **1993**, *36*, 2842–2844.

(20) Awaya, N.; Arita, Y. *Jpn. J. Appl. Phys. Pt. 1* **1993**, *32*, 3915.

(21) Chang, Y. N. In *Evolution of Surface and Thin Film Microstructure*; Material Research Society: Pittsburgh, 1983; pp 649–652.

(22) Chiang, C. M.; Miller, T. M.; Dubois, L. H. *J. Phys. Chem.* **1993**, *97*, 11781–11786.

(23) Dubois, L. H.; Zegarski, B. R. *J. Electrochem. Soc.* **1992**, *139*, 3295–3299.

(24) Gelatos, A. V.; Jain, A.; Marsh, R.; Mogab, C. J. *MRS. Bull.* **1994**, *19*, 49–54.

(25) Lecohier, B.; Calpini, B.; Philippoz, J. M.; Vandenberg, H. *J. Appl. Phys.* **1992**, *72*, 2022–2026.

(26) Lecohier, B.; Calpini, B.; Philippoz, J. M.; Vandenberg, H.; laub, D.; Buffat, P. A. *J. Electrochem. Soc.* **1993**, *140*, 789–796.

(27) Stumm, T. H.; Vandenberg, H. *Mater. Sci. Eng. B: Solid State Mater. Adv. Technol.* **1994**, *23*, 43–53.

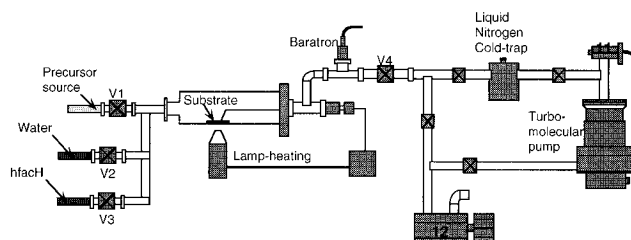


Figure 1. Cold-wall turbomolecular pumped differential reactor.

In this work, we set out to develop an understanding of the reaction pathway for CVD of Cu using (hfac)Cu(VTMS) and (hfac)Cu(2-butyne) in the presence of water, including (i) hot-wall CVD of Cu to determine the overall CVD pathway for (hfac)CuL in the presence of water vapor, (ii) deposition rate measurements of (hfac)Cu(VTMS) and (hfac)Cu(2-butyne) as a function of water vapor flow rate to identify the rate-limiting reaction, (iii) studies of the CVD of Cu using (hfac)Cu(VTMS) as a function of water, methanol, and dimethyl ether vapor flow rates to identify the reason for deposition rate enhancement, (iv) identification of the impurity phases in the films formed using (hfac)Cu(VTMS) as a function of water vapor flow rate, (v) determination of the reaction pathways resulting in impurity incorporation, and (vi) development of strategies for deposition of high-purity Cu in the presence of water to take advantage of the rate enhancement.

Experimental Section

The experimental setups consisted of a cold-wall and a hot-wall CVD reactor. Figure 1 shows a schematic diagram of the cold-wall CVD reactor designed for measurement of the deposition rate outside the feed-rate-limited regime by allowing less than 2–3% precursor conversion. This was achieved by operating at temperature low enough to give small reaction efficiencies of the precursor. The conversion was quantified by measuring the mass increase of the substrate and converting this to a mass of precursor. This mass was compared with the total mass of transported precursor. The substrate (silicon wafer with a ~1000 Å layer of CVD tungsten) was lamp-heated, and the temperature was measured by a thermocouple on the substrate surface. This system has been described in more detail previously.¹⁴

The cold-wall CVD reactor was converted to a hot-wall reactor for studying the product distribution during CVD. The lamp heater was replaced by heating tapes wrapped around the reactor walls to increase the surface area for deposition and promote ~100% precursor conversion at the reactor walls. The deposition temperature was measured by placing a thermocouple in contact with the outside wall of the reactor chamber while avoiding contact with the heating tape. The thermocouple was covered with insulation which was in turn wrapped with heating tape. Thus, the measured temperature was that of the outside surface of the glass reactor. Considering the low heat-transfer rates inside the reactor, the temperatures inside and outside the reactor wall should have been nearly identical. Also, because all the precursor was reacted, any errors in temperature measurement would have had an inconsequential impact on the result.

The CVD of copper was studied for (hfac)Cu(VTMS) (Schumacher) at a flow rate of 2 sccm and substrate temperature of 160 °C and for (hfac)Cu(2-butyne) at a flow rate of 10 sccm and substrate temperature of 150 °C. Different temperatures were required because of the different reaction rates of the two precursors. The source vessels for the precursor and additional reagents were held at room temperature and their vapor flow rates controlled by needle valves V1 and V2 or V3 respectively. The throttle valve V4 was fully opened to

Table 1. Summary of the CVD Conditions and the Copper Yields in the Hot-Wall Reactor for (hfac)Cu(VTMS) and (hfac)Cu(2-butyne) as a Function of Water Vapor Flow Rate

precursor/flow rate (sccm)	water vapor flow rate (sccm)	chamber pressure (mTorr)	deposition temp (°C)	copper yield (%)
(hfac)Cu(VTMS) (2 sccm)	0.2 (low)	12	160	50
	2.4 (high)	23	160	52
(hfac)Cu(2-butyne) (10 sccm)	0.2 (low)	11	150	50
	1.2 (high)	19	150	53

maintain a constant pumping speed and the corresponding chamber pressure was measured by a capacitance manometer. These CVD conditions were common to all the experiments.

The deposition rate and resistivity were measured for films deposited in the cold-wall reactor. The deposition rate was estimated by calculating film thickness from the weight gain of the substrate after deposition, and the resistivity was calculated from the film resistance measured by a four-point probe. No induction period was observed suggesting that the nucleation process had no effect on measured deposition rates. The film purity was evaluated by X-ray photoelectron spectroscopy (XPS) to identify impurity phases and their percentage incorporation in the films. Some films were also analyzed by secondary ion mass spectroscopy (SIMS) for quantitative elemental analysis. The most important concerns were the presence of copper oxide phases in addition to elemental impurities such as C, O, F, and Si.

Overall CVD Pathway in the Presence of Water. Copper deposition was studied in the hot-wall reactor using (hfac)Cu(VTMS) and (hfac)Cu(2-butyne) in the presence of water vapor to determine whether the overall CVD pathway is identical with that in the absence of water. The water vapor flow rates using (hfac)Cu(VTMS) were 0.2 (low) and 2.4 (high) sccm and the corresponding chamber pressures were 11 and 23 mTorr, respectively. The water vapor flow rates using (hfac)Cu(2-butyne) were 0.2 (low) and 1.2 (high) sccm and the corresponding chamber pressures were 11 and 19 mTorr, respectively. Table 1 summarizes the hot-wall CVD reactor conditions for the two precursors.

The hot-wall experiments allowed determination of the maximum copper yield for CVD in the presence of water vapor. This was determined by the mass of copper deposited on the reactor walls by measuring the weight increase (using a four decimal place weighing balance) of the detachable quartz reactor tube after deposition (total weight ~120 g) and calculating the copper yield for a known mass flow rate of the precursor. The volatile reaction products were cold-trapped and analyzed by nuclear magnetic resonance (¹H and ¹³C NMR) for identification of possible decomposition fragments of the "hfac" species.

Cold-Wall CVD of Cu in the Presence of Water. The deposition rate was measured using (hfac)Cu(VTMS) and (hfac)Cu(2-butyne) in the cold-wall reactor as a function of water vapor flow rate and constant substrate temperature and precursor flow rate. The deposition rate enhancements for the two precursors were compared to gain insight into the rate-limiting reaction. The water vapor flow rate was varied from 0.2 and 2.4 sccm over the range of the study.

Deposition Rate Enhancement Using (hfac)Cu(VTMS) in the Presence of Water. Films were deposited using (hfac)Cu(VTMS) in the presence of deionized water (H-O-H), methanol (Me-O-H, semiconductor grade, V.W.R., dried over Mg), and dimethyl ether (Me-O-Me, Johnson Mathey, 99.9% purity, used as received) in a cold-wall reactor to observe the effect of systematic reduction in the number of active protons attached to the oxygen in the added reagents on the deposition rate. The methanol vapor flow rate ranged from 0.5 to 8 sccm and the corresponding chamber pressure varied from 10 to 17 mTorr. The dimethyl ether vapor flow rate ranged from 2 to 12 sccm and the corresponding chamber pressure varied from 11 to 18 mTorr.

Film Morphology and Impurities in Films Deposited in the Presence of Water. The film morphology was evaluated from the scanning electron micrographs (SEM). The films were analyzed by XPS and SIMS for the presence of impurity phases, oxidation state, and quantitative elemental

analysis. The impurity incorporation was also investigated by using isotopically labeled water (H₂¹⁸O, Isotech) with 10.7% ¹⁸O enrichment. The films were deposited using (hfac)Cu(VTMS) and (hfac)Cu(2-butyne) in the presence of H₂¹⁸O vapor under the same conditions used for H₂¹⁶O. The films were then analyzed by SIMS (Cameca IMS 4f).

Pathway for Impurity Incorporation in the Presence of Water. The reaction of Cu(hfac)₂ (reaction product of the CVD of Cu reaction (eq 1) and water vapor in a cold-wall reactor was studied to determine if their interaction could result in the formation of copper oxides. Two substrates were used, one consisting of a ~1000 Å layer of CVD tungsten and the other consisting of a ~3000 Å layer of Cu deposited by sputtering. The source vessels for Cu(hfac)₂ and water were kept at room temperature. A Cu(hfac)₂ flow rate of 2 sccm was used, and the other conditions of water vapor flow rate, substrate temperature, and chamber pressure were those used for the study using (hfac)Cu(VTMS) in the presence of water. The CVD experiments were carried out for intervals of 3, 5, and 15 min. The weight gain and the resistance were measured after deposition on both substrates. The films were then analyzed by X-ray diffraction (XRD) to identify which copper oxide phase was present. The observed weight increase corresponded to deposition of material and could not be accounted for by oxidation of the original copper layer.

The films were then exposed to hfach vapor at a substrate temperature of 200 °C, 5 sccm hfach flow rate, and chamber pressure of 23 mTorr for 15 min. The hfach has been shown to etch copper oxide under these conditions.^{28,29} The extent of etching of the film deposited from Cu(hfac)₂ and water could be determined by observing a decrease in the weight of the substrate and if it occurred would suggest a pathway for incorporation of copper oxides in the Cu films via reaction of Cu(hfac)₂ and water on the surface.

Suppressing Impurities in Films Deposited in the Presence of Water. Deposition using (hfac)Cu(VTMS) was studied for simultaneous flow of water and hfach vapor. The hfach vapor was introduced during CVD to suppress the incorporation of copper oxide in the Cu films. The source vessel for the hfach was held at room temperature and the vapor flow rate controlled by needle valve V3. The CVD was done at water vapor flow rates of 0.2 (low) and 2.4 (high) sccm and 0.4 sccm hfach flow rate. The chamber pressures corresponding to the two conditions were 14 (0.3 sccm water) and 19 mTorr (2.4 sccm water), respectively. The deposition rate and resistivity were measured and the films were analyzed by SIMS.

X-ray Crystallographic Study of Cu(hfac)₂·H₂O. The sample of Cu(hfac)₂·H₂O used for single-crystal X-ray diffraction analysis was prepared by sublimation. A summary of the crystal data and experimental details is presented in Table 2. The crystallographic data were obtained at 293 K with a 2θ range of 3.0–50.0° with ω-scan type. The structure was solved by direct methods. The systematic absences in the diffraction data are uniquely consistent for the space group *P2₁/c*. Initially all *F*'s were refined with a two-site positional disorder model in CF₃ groups. Refinement with all hydrogen atoms included in idealized positions (riding model) resulted in location of water hydrogens which were adjusted to 0.85 Å from O(5). Another refinement with all hydrogen atoms included and no disorder on *F*'s but with *F*'s allowed anisotropic *U*'s

(28) Rousseau, F.; Jain, A.; Kodas, T. T.; Hampden-Smith, M. J.; Farr, J. D.; Muenchausen, R. *J. Mater. Chem.* **1992**, *2*, 893.

(29) Jain, A.; Kodas, T.; Hampden-Smith, M. *Thin Solid Films* **1995**, *269*, 51–56.

Table 2. Summary of Crystal Data for Cu(hfac)₂(H₂O)^a

empirical formula	C ₁₀ H ₄ CuF ₁₂ O ₅
F.W.	495.7
color, habit	pale blue-green plates
unit cell, dimension	
<i>a</i> (Å)	11.083(2)
<i>b</i> (Å)	6.654(1)
<i>c</i> (Å)	21.816(4)
β (deg)	90.46(3)
crystal system	monoclinic
space group	<i>P</i> 2 ₁ / <i>c</i>
<i>T</i> /K	293
$\lambda/\text{Å}$	0.71073
<i>Z</i>	4
crystal size/mm	0.121 × 0.276 × 0.805
volume (Å ³)	1608.6(5)
reflns collected	9856
reflns used	2662
abs coeff/mm ⁻¹	1.511
<i>R</i> (<i>F</i>) %*	6.09
<i>R</i> _w (<i>F</i>) %	6.45

$$^a R = \sum \Delta F / \sum F_o, R_w = \sum W^{1/2} \Delta F / \sum W^{1/2} F_o.$$

Table 3. Atomic Coordinates (×10⁴) and Equivalent Isotropic Displacement Coefficients (Å² × 10³) for Cu(hfac)₂·H₂O^a

	<i>x</i>	<i>y</i>	<i>z</i>	<i>U</i> (eq)
Cu	2791(1)	934(1)	7153(1)	45(1)
O(1)	1542(3)	2312(7)	7601(2)	49(1)
O(2)	3145(3)	-823(7)	7844(2)	52(1)
C(1)	1114(5)	1731(10)	8103(3)	45(2)
C(2)	1517(5)	187(11)	8469(3)	50(2)
C(3)	2503(5)	-953(11)	8315(3)	45(2)
C(4)	24(7)	2946(15)	8301(3)	70(3)
F(1)	-197(5)	2855(12)	8872(2)	133(3)
F(2)	174(6)	4886(11)	8200(3)	132(3)
F(3)	-908(4)	2505(13)	7990(3)	150(4)
C(5)	2897(6)	-2643(12)	8740(3)	60(3)
F(4)	2283(6)	-2823(12)	9235(3)	145(3)
F(5)	4020(4)	-2553(9)	8876(3)	118(3)
F(6)	2777(7)	-4408(9)	8470(3)	130(3)
O(3)	3822(4)	-827(8)	6679(2)	55(2)
O(4)	2152(3)	2212(7)	6416(2)	52(2)
C(6)	3787(5)	-992(10)	6106(3)	45(2)
C(7)	3106(6)	91(12)	5696(3)	56(2)
C(8)	2350(5)	1604(11)	5885(3)	47(2)
C(9)	4591(7)	-2671(14)	5871(3)	66(3)
F(7)	5630(4)	-2695(11)	6130(3)	133(3)
F(8)	4761(8)	-2666(16)	5296(3)	194(5)
F(9)	4166(7)	-4417(10)	5991(5)	160(4)
C(10)	1620(7)	2733(17)	5392(4)	76(4)
F(10)	1939(7)	2442(17)	4861(2)	200(5)
F(11)	501(5)	2392(18)	5441(4)	188(5)
F(12)	1655(9)	4649(14)	5465(4)	184(5)
O(5)	4227(4)	3163(10)	7365(2)	85(2)

^a Equivalent isotropic *U* defined as one-third of the trace of the orthogonalized *U*_{ij} tensor.

resulted in much lower *R* values. All software and the source of scattering factors are contained in the SHELXTL program library (G. Sheldrick, Nicolet Corp., Madison, WI). Atomic coordinates are presented in Table 3 and bond lengths and angles in Tables 4 and 5, respectively. An ORTEP plot emphasizing the hydrogen-bonded structure of Cu(hfac)₂·H₂O is shown in Figure 6.

Results and Discussion

Overall CVD of Cu Pathway in the Presence of Water. The maximum copper yield from complete conversion of (hfac)CuL via disproportionation can only be 50% for CVD of Cu according to eq 1. The hot-wall CVD using (hfac)Cu(VTMS) and (hfac)Cu(2-butene) at low water flow rate (Table 1) resulted in a copper yield of 50% within the limits of the experimental error

Table 4. Relevant Bond Lengths for Cu(hfac)₂·H₂O

Cu–O(1)	1.932 (4)	Cu–O(2)	1.944 (5)
Cu–O(3)	1.942 (5)	Cu–O(4)	1.947 (4)
Cu–O(5)	2.221 (6)	O(1)–C(1)	1.258 (7)
O(2)–C(3)	1.258 (7)	C(1)–C(2)	1.374 (9)
C(1)–C(4)	1.519 (10)	C(2)–C(3)	1.373 (9)
C(3)–C(5)	1.520 (10)	C(4)–F(1)	1.273 (9)
C(4)–F(2)	1.321 (12)	C(4)–F(3)	1.266 (9)
C(5)–F(4)	1.286 (9)	C(5)–F(5)	1.279 (8)
C(5)–F(6)	1.320 (10)	O(3)–C(6)	1.255 (7)
O(4)–C(8)	1.249 (7)	C(6)–C(7)	1.371 (9)
C(6)–C(9)	1.520 (11)	C(7)–C(8)	1.375 (10)
C(8)–C(10)	1.537 (11)	C(9)–F(7)	1.278 (9)
C(9)–F(3)	1.269 (10)	C(9)–F(9)	1.282 (11)
C(10)–F(10)	1.230 (10)	C(10)–F(11)	1.265 (10)
C(10)–F(12)	1.286 (15)		

Table 5. Relevant Bond Angles for Cu(hfac)₂·H₂O

O(1)–Cu–O(2)	92.0(2)	O(1)–Cu–O(3)	169.5(2)
O(2)–Cu–O(3)	86.2(2)	O(1)–Cu–O(4)	87.3(3)
O(2)–Cu–O(4)	166.5(2)	O(3)–Cu–O(4)	92.0(2)
O(1)–Cu–O(5)	95.3(2)	O(2)–Cu–O(5)	95.8(2)
O(3)–Cu–O(5)	95.2(2)	O(4)–Cu–O(5)	97.8(2)
Cu–O(1)–C(1)	124.8(4)	Cu–O(2)–C(3)	124.3(4)
O(1)–C(1)–C(2)	127.8(6)	O(1)–C(1)–C(4)	113.0(6)
C(2)–C(1)–C(4)	119.3(6)	O(2)–C(3)–C(2)	128.1(6)
C(1)–C(2)–C(3)	121.8(6)	C(2)–C(3)–C(5)	119.0(6)
O(2)–C(3)–C(5)	112.8(5)	C(1)–C(4)–F(2)	111.8(6)
C(1)–C(4)–F(1)	114.4(7)	C(1)–C(4)–F(3)	111.8(7)
F(1)–C(4)–F(2)	103.6(8)	F(2)–C(4)–F(3)	103.9(8)
F(1)–C(4)–F(3)	110.6(7)	C(3)–C(5)–F(5)	112.4(6)
C(3)–C(5)–F(4)	115.4(7)	C(3)–C(5)–F(6)	111.1(6)
F(4)–C(5)–F(5)	109.3(6)	F(5)–C(5)–F(6)	103.9(7)
F(4)–C(5)–F(6)	103.8(7)	Cu–O(4)–C(8)	124.0(4)
Cu–O(3)–C(6)	124.8(4)	C(3)–C(6)–C(9)	112.7(6)
O(3)–C(6)–C(7)	128.0(6)	C(6)–C(7)–C(8)	121.6(6)
C(7)–C(6)–C(9)	119.2(6)	O(4)–C(8)–C(10)	113.3(6)
O(4)–C(8)–C(7)	128.8(6)	C(6)–C(9)–F(7)	112.9(7)
C(7)–C(8)–C(10)	117.8(6)	F(7)–C(9)–F(8)	107.2(8)
C(6)–C(9)–F(8)	115.0(8)	F(7)–C(9)–F(9)	103.3(8)
C(6)–C(9)–F(9)	112.3(7)	C(8)–C(10)–F(10)	115.4(8)
F(8)–C(9)–F(9)	105.2(9)	F(10)–C(10)–F(11)	110.0(8)
C(8)–C(10)–F(11)	111.3(8)	F(10)–C(10)–F(12)	105.3(10)
C(8)–C(10)–F(12)	112.5(8)	F(11)–C(10)–F(12)	101.3(10)

(~0.5%). This supports the idea that the overall CVD pathway using (hfac)CuL in the *presence* of water also occurs primarily via eq 1 for CVD in the *absence* of water. In contrast, the yields for the two precursors at high water flow rates were only 2–3% above the maximum copper yield of 50% predicted by eq 1. This supports the idea that the majority of the material was deposited by disproportionation. The 2–3% additional yield may be the result of impurity incorporation (O) in the films rather than pure copper as shown later.

Cold-Wall CVD of Cu in the Presence of Water.

Deposition using (hfac)CuL in the *absence* of water suggested that the dissociation of L from (hfac)CuL could be the rate-limiting surface reaction under surface-reaction-limited conditions. In the *presence* of water, the reactions given by eqs 3 and 4 are likely to be affected and may proceed differently because water is also a potential donor ligand analogous to L. The adsorption and desorption characteristics of the precursor, Cu(hfac)₂, and L on the copper surface (eqs 2, 5 and 6) are not likely to change in the presence of water because they are adsorbent–adsorbate interactions. However, water could compete for surface sites thereby influencing the kinetics. Because the desorption of Cu(hfac)₂ (eq 5) and VTMS (eq 6) were likely not rate-limiting during CVD of Cu for deposition rates of up to ~1 μm/min in the absence of water, we presume that

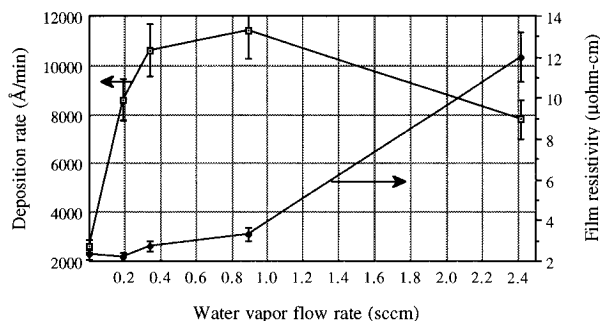


Figure 2. Deposition rate and resistivity as a function of water vapor flow rate using (hfac)Cu(VTMS) at a substrate temperature of 160 °C.

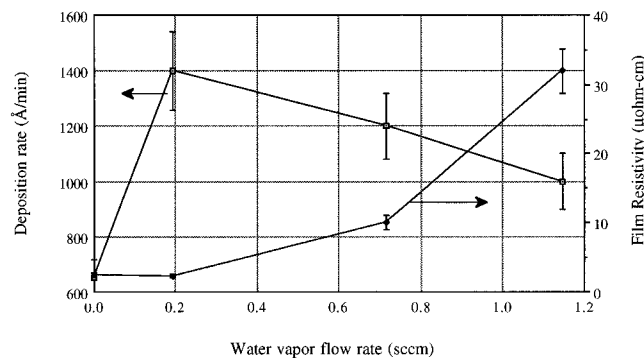


Figure 3. Deposition rate and resistivity as a function of water vapor flow rate using (hfac)Cu(2-butyne) at a substrate temperature of 150 °C.

these steps are less likely to be affected by the presence of water.

Figures 2 and 3 show the deposition rate as a function of water vapor flow rate for (hfac)Cu(VTMS) and (hfac)Cu(2-butyne), respectively. The conditions were outside the feed-rate-limited regime, similar to the conditions in the *absence* of water. The deposition rate increased by a maximum factor of 4 for (hfac)Cu(VTMS) and by a maximum factor of 2 for (hfac)Cu(2-butyne) compared to deposition in the absence of water. The extent of the deposition rate enhancement was different for the two precursors which supports the idea that the dissociation of the neutral ligand from the parent molecule (eq 3) is still involved in the rate-limiting step. Equation 3 involves cleavage of the Cu–L bond, and the observed differences in the rate enhancements could be the result of the differences in the bond strengths or lability of Cu–(VTMS) vs Cu–(2-butyne). This result is also consistent with the difference in activation energies for the deposition of copper from these precursors in the absence of water. The disproportionation reaction (eq 4) is not likely to be rate-limiting because it is independent of the nature of the neutral ligand and should have resulted in similar deposition rate enhancements for both precursors.

Deposition Rate Enhancement Using (hfac)Cu(VTMS) in the Presence of Water. An understanding of the nature of the Cu–VTMS bonding is important in explaining the enhancement in deposition rate. The Cu–VTMS bond in (hfac)Cu(VTMS) is formed as a result of electron donation by VTMS to the copper, and there is little evidence for π -backbonding from copper to the ligand (as determined by the metrical parameters

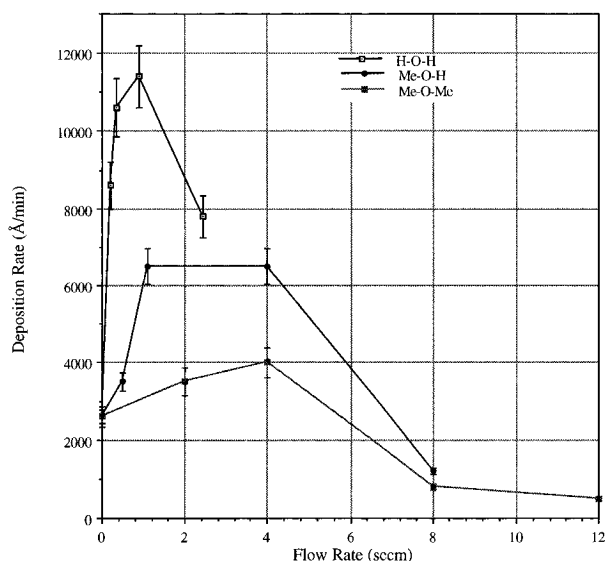


Figure 4. Deposition rates using (hfac)Cu(VTMS) as a function of water, methanol, and dimethyl ether vapor flow rates at a substrate temperature of 160 °C.

of the ligand).³⁰ As a result, the Cu–VTMS bond could be weakened in the *presence* of water by hydrogen bridging between the oxygen in the “hfac” ring and the hydrogen in the water molecule and/or by the electron donation by the oxygen in the water molecule to the copper center to form a 4-coordinate intermediate as one extreme. These interactions are likely to destabilize the Cu–VTMS bond by satisfying the coordinative and electronic unsaturation of copper(I). To determine the dominant interaction, comparative studies of the deposition rate were made in the presence of water (H–O–H), methanol (Me–O–H), and dimethyl ether (Me–O–Me). The use of H₂O, MeOH, and MeOMe allowed a systematic study of the effect of decreasing the number of active protons (H) and replacing them by methyl groups (Me).

The reduction in the number of active protons available in the added reagents decreased the hydrogen-bonding interactions to zero, while replacement of the active proton by methyl groups increased the electron-donating ability of oxygen to the copper due to the higher donor ability of the methyl group. If hydrogen-bonding effects play a dominant role in destabilizing the Cu–VTMS bond, the deposition rate enhancement for CVD of Cu should be highest in the presence of H₂O followed by MeOH and MeOMe and vice versa if the electron-donor ability dominates. Steric effects may complicate these issues by limiting the steric accessibility of the added reagents to the β -diketonate oxygen or the copper center.

Figure 4 shows the deposition rate for CVD of Cu using (hfac)Cu(VTMS) as a function of vapor flow rate of water, methanol, and dimethyl ether. The deposition rate enhancement is highest for water followed by MeOH and MeOMe, suggesting that hydrogen bonding plays a dominant role in destabilizing the Cu–VTMS bond, resulting in the observed deposition rate enhancement. However, the influence of the increased steric demands of Me₂O over H₂O cannot be distinguished in this study. It is likely that both the hydrogen-bonding

(30) Norman, J. A. T.; Muratore, B. A.; Dyer, P. N.; Roberts, D. A.; Hochberg, A. K.; Dubois, L. H. *Mater. Sci. Eng. B* **1993**, *17*, 87.

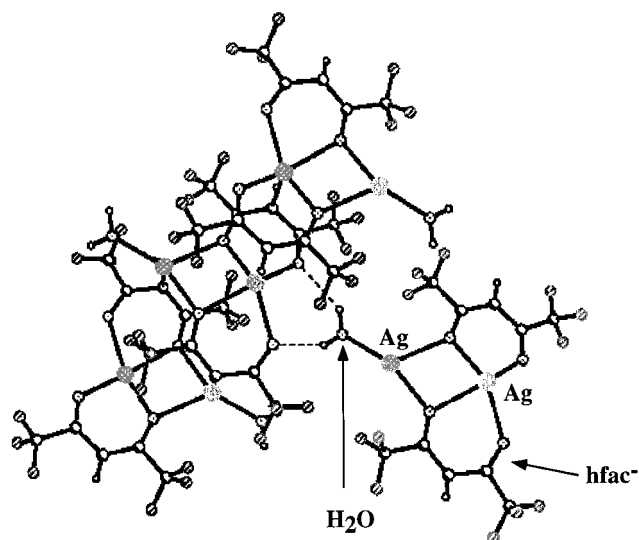


Figure 5. Crystal structure of $[(\text{hfac})\text{Ag}]_2(\text{H}_2\text{O})$ emphasizing the coordination of the water molecule.

ability and the donor ability of the oxygen atom contribute to destabilization of the Cu–L bond.

Evidence for both hydrogen bonding of water to hfac ligands and donation of an oxygen lone pair in water to a group 11 metal center exists in the literature in the solid state. For example the structure of $[(\text{hfac})\text{Ag}]_2(\text{H}_2\text{O})$ was recently reported in which the water ligand was bonded through oxygen to one silver(I) center and hydrogen-bonded to oxygen atoms of the hfac ligand in adjacent molecules in the solid state, as shown in Figure 5.³¹ As part of this work, we have determined the solid-state structure of $\text{Cu}(\text{II})(\text{hfac})_2(\text{H}_2\text{O})$ since $\text{Cu}(\text{I})(\text{hfac})(\text{H}_2\text{O})$ is too thermally unstable (with respect to disproportionation) to be isolated. The crystal data and metrical parameters are presented in Tables 2–5. The bonding mode of the water ligand is analogous to the silver(I) water adduct in that the oxygen atom of the water ligand is datively bonded to $\text{Cu}(\text{II})$ and hydrogen-bonded to oxygen atoms of an adjacent $\text{Cu}(\text{hfac})_2$ molecule as shown in Figure 6. However, the structure of $\text{Cu}(\text{hfac})_2 \cdot \text{H}_2\text{O}$ determined here differs somewhat from that recently described in the literature.³² While the molecular structures of the two species are similar, the crystal structures exhibit different intermolecular hydrogen-bonding arrangements. This could be due to the different temperatures at which the X-ray data were collected. The important point is that formation of a donor bond between OH_2 and the Cu center together with H-bonding are important structural features.

It is interesting to note that dimethyl ether enhances the deposition rate but does not have an active proton with which to hydrogen-bond or react with the hfac ligand. The purity of the films deposited with MeOH and MeOMe as indicated by resistivity measurements could provide an indication of the extent of impurity phase incorporation, but measured resistivity values ($2.2\text{--}7 \mu\Omega \text{ cm}$) could have been influenced by the morphology of the films. As a result, a conclusion cannot be drawn from resistivity data as to the forma-

tion of phases like Cu_2O as a function of the coreactant (H_2O , MeOH, and MeOMe).

Film Morphology and Impurities in CVD of Cu Films in the Presence of Water. The addition of water had an effect on the morphology, resistivity, and purity of the films for both $(\text{hfac})\text{Cu}(\text{VTMS})$ and $(\text{hfac})\text{Cu}(2\text{-butyne})$. At low water vapor flow rate of 0.2 sccm the films exhibited a copper color, near bulk resistivities ($\sim 2.0 \mu\Omega \text{ cm}$) (Figures 2 and 3) and were smoother than in the absence of water (Figures 7 and 8). The films exhibited a dark brown color and increased resistivity (Figures 2 and 3) and were more porous at high water vapor flow rates (Figures 7 and 8).

A SIMS analysis [detection limit of parts per million (ppm)] was carried out to detect low levels of elemental impurities in the films. The reference used was sputter-deposited Cu (purchased from Matheson, 99.999% pure). The data reported in Table 6 are the counts per peak, that is, the total accumulated counts for each element. The numbers can be compared qualitatively because the samples had similar major element composition (i.e., same matrix) and the same beam current was used on each sample. The analysis showed the presence of some fluorine (F) in the films deposited at optimum water vapor flow rate and the presence of oxygen (O) and fluorine (F) in the films deposited at high water vapor flow rates. The hydrogen content was not investigated. Table 6 summarizes the XPS and SIMS analysis on Cu films deposited by $(\text{hfac})\text{Cu}(\text{VTMS})$. Similar trends were observed for Cu films deposited by $(\text{hfac})\text{Cu}(2\text{-butyne})$. The absence of Si and C in the films suggests that both neutral ligands (VTMS and 2-butyne) desorb molecularly from the surface without reacting with the water.

The source of the small amounts of fluorine in the films is likely to be due to a small amount of decomposition of the hfac ligand because the hfac fragment is the only source of F. However, the presence of fluorine (F) in the films is inconsistent with the NMR ^{13}C analysis which showed an absence of decomposition fragments of hfac ligand in the cold-trapped reaction products. This may, however, be due to the relatively poor sensitivity of NMR relative to SIMS. The presence of F is also inconsistent with the lack of C in the films which can be explained only if the carbon-containing fragments preferentially desorb. An alternate explanation could be that some unidentified volatile fluorine species was present in the precursor after synthesis and remained dissolved in the precursor at low levels even after purification. However, no direct evidence is available to support this possibility.

The XPS analysis (detection limit $\sim 1 \text{ at. } \%$) was carried out to identify impurity phases in the films deposited at the optimum and higher water vapor conditions for both precursors. The films deposited at the optimum water vapor flow rate were pure within the detection limits of XPS but showed the presence of oxygen in the form of copper(I) oxide (Cu_2O) [$\sim 2\text{--}3 \text{ at. } \%$] for high water vapor flows. Fluorine, carbon, and silicon were undetected by XPS at both the optimum and high water vapor conditions, showing that these elements were either not present or below the detection limit.

The presence of oxygen in the form of copper(I) oxide in films deposited at high water flow rates suggested a

(31) Xu, C.; Corbitt, T.; Hampden-Smith, M. J.; Kudas, T. T.; Duesler, E. N. *J. Chem. Soc., Dalton Trans.* **1994**, 2841–2849.

(32) Pinkas, J.; Huffman, J. C.; Baxter, D. V.; Chisholm, M. H.; Caulton, K. G. *Chem. Mater.* **1995**, 7, 1589–1596.

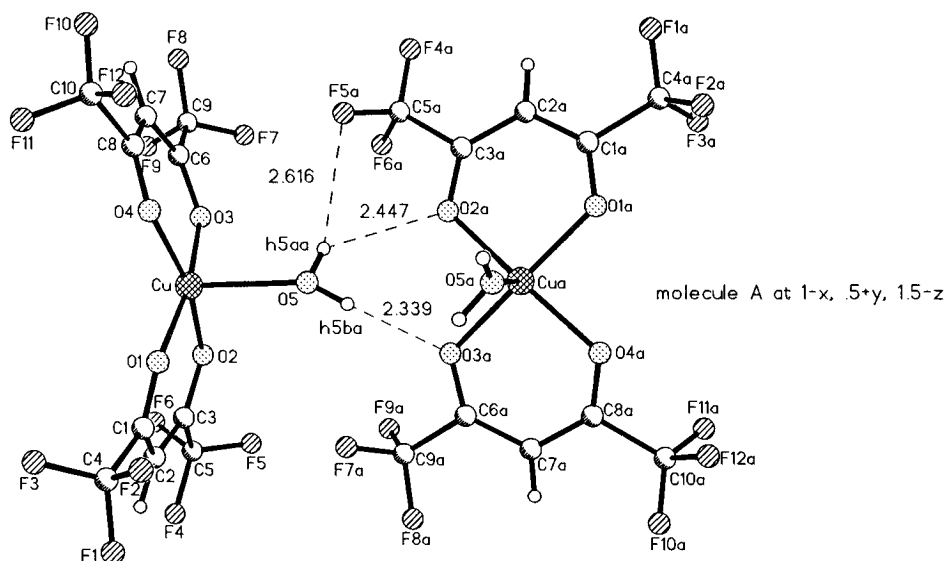


Figure 6. Crystal structure of $\text{Cu}(\text{hfac})_2(\text{H}_2\text{O})$ emphasizing the coordination of the water molecule.

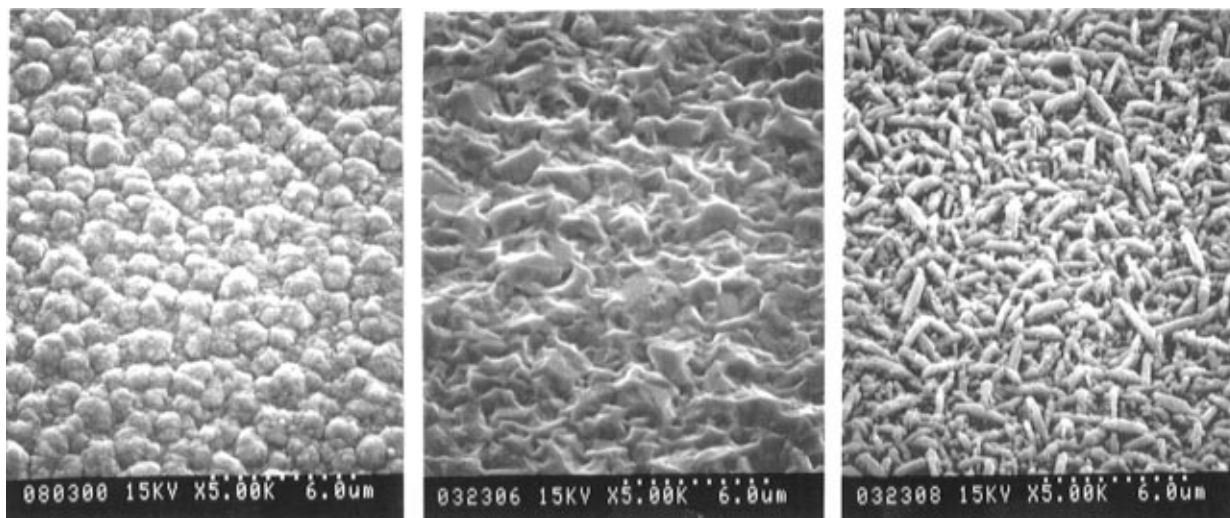


Figure 7. Films deposited using $(\text{hfac})\text{Cu}(\text{VTMS})$ showing the effect of water on film morphology: (left) no water, (middle) optimum water flow rate (0.2 sccm), and (right) high water flow rate (2.4 sccm).

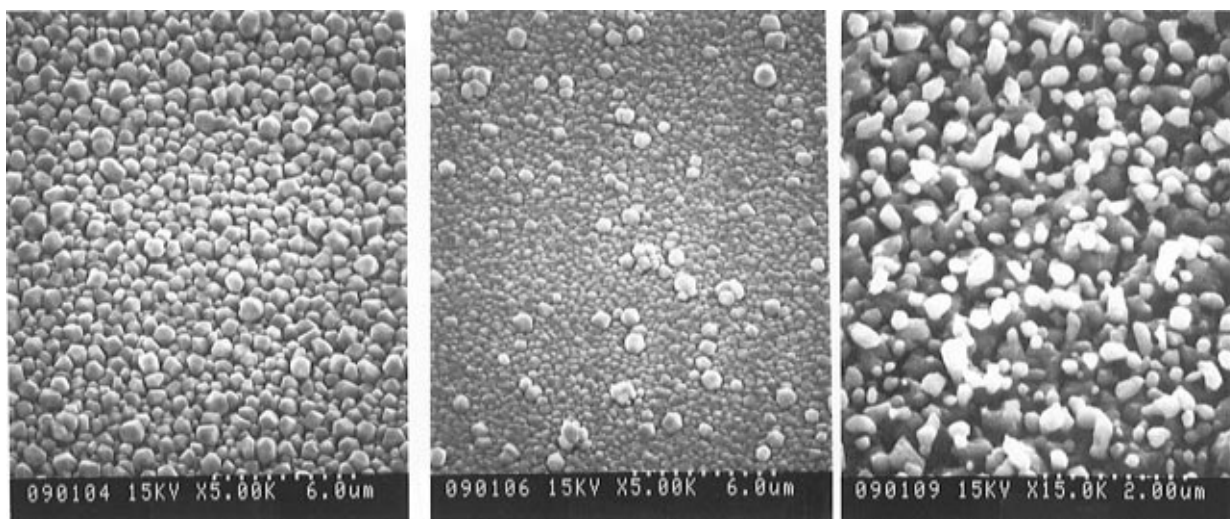


Figure 8. Films deposited using $(\text{hfac})\text{Cu}(2\text{-butyne})$ showing the effect of water on film morphology: (left) no water, (middle) optimum water flow rate (0.2 sccm), and (right) high water flow rate (1.2 sccm).

reaction involving water and $\text{Cu}(\text{hfac})_2$ (the only reactive disproportionation reaction product) or intermediates leading to its formation. The possibility of a reaction involving water was also supported by the observed

increase in the mole fraction of Cu_2O in the film with water vapor flow rate despite no further increase in deposition rate above the optimum water levels (Figures 4 and 5).

Table 6. Summary of the XPS and SIMS Analysis of the Films Deposited Using (hfac)Cu(VTMS) as a Function of Water Vapor Flow Rate

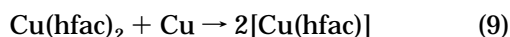
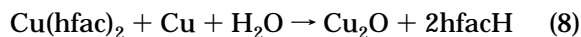
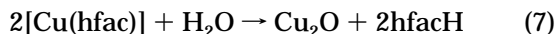
	optimum water vapor flow rate	higher water vapor flow rate	sputter-deposited Cu
XPS analysis	pure Cu within detection limit	1–2% Cu ₂ O phase present	pure Cu within detection limit
SIMS analysis	C, ~10 ³ O, ~10 ³ F, ~10 ⁴ Si, ~10 ¹	C, ~10 ³ O, ~10 ⁶ F, ~10 ⁵ Si, ~10 ¹	C, ~10 ³ O, ~10 ³ F, ~10 ¹ Si, ~10 ³

Table 7. Summary of the XPS and SIMS Analysis of the CVD of Cu Films Deposited Using (hfac)Cu(VTMS) at High Water Vapor Flow Rate (2.4 sccm) with and without Flow of hfach Vapor (0.4 sccm)

	high water vapor flow rate	high water vapor flow rate along with Hfach	sputter-deposited Cu
XPS analysis	1–2% Cu ₂ O phase present	pure Cu within detection limit	pure Cu within detection limit
SIMS analysis	C, ~10 ³ O, ~10 ⁶ F, ~10 ⁵ Si, ~10 ¹	C, ~10 ³ O, ~10 ³ F, ~10 ⁴ Si, ~10 ¹	C, ~10 ³ O, ~10 ³ F, ~10 ¹ Si, ~10 ¹

To determine whether water was the source of the oxygen in the films and to exclude the possibility of the hfac ligand as the source, isotopically labeled oxygen in the form ~10% enriched H₂¹⁸O was used for a CVD experiment and the ¹⁸O content of the film analyzed by SIMS. The SIMS analysis confirmed qualitatively the presence of at least an order of magnitude higher ¹⁸O concentration above its natural abundance in the Cu films for both precursors supporting the idea that water was one of the reactants leading to formation of Cu₂O in the Cu films.

Pathway for Impurity Incorporation in CVD of Cu Films in the Presence of Water. A possible pathway for copper(I) oxide incorporation during CVD of Cu is via reaction of surface-bonded [Cu(hfac)] and H₂O according to eq 7. It is unlikely that Cu₂O would



be formed as the only product of the reaction between Cu(hfac)₂ and water in the absence of copper as supported by a recent study which also showed ligand oxidation products.³² However, in the presence of Cu, Cu(hfac)₂ reacts to form surface [Cu(hfac)] species; therefore, a more general equation can be written such as that presented in eq 8 based on the reversibility of the disproportionation reaction, eq 9. This suggests that it should be possible to deposit Cu₂O by reaction of Cu(hfac)₂ and H₂O on a copper surface under conditions similar to CVD of Cu.

Deposition experiments using Cu(hfac)₂ and H₂O at the deposition temperature of 170 °C on a copper substrate resulted in the formation of a dark brown film on the Cu surface. Film growth was self-limiting and stopped after ~300–400 Å. This can be explained by realizing that one of the reactants is copper (eq 8) and the surface coverage by the Cu₂O film stops the Cu(hfac)₂ and H₂O molecules from reaching the Cu surface, thereby inhibiting the reaction. The CVD temperature (<200 °C) was not high enough to allow enough copper diffusion through the film to reach the top surface or

allow decomposition of Cu(hfac)₂ for continued growth of the film. The self-limiting thickness was significantly greater than a few monolayers because the film exhibited a porous structure which allowed Cu(hfac)₂ and H₂O molecules to reach the copper surface.

The powder X-ray diffraction analysis of the film deposited on the Cu surface showed that the film was copper(I) oxide. The presence of Cu₂O was also supported by the ability to subsequently etch the film by reaction with hfach (reverse reaction of eq 8). Studies on dry etching of copper oxides have shown that hfach etches copper(I) oxide (not copper metal) according to the reverse reaction shown in eq 7.²⁸ The weight loss of the etched film was approximately half the weight of Cu₂O film because of the formation of Cu as an etch product, also consistent with the etching reaction.

In a control experiment, CVD using Cu(hfac)₂ and H₂O was also carried out on a tungsten surface under the same conditions. No deposition was observed even after 1 h, confirming the need for Cu in this surface reaction. These results are in contrast to a recent study of the deposition of Cu₂O films from Cu(hfac)₂ and H₂O, which was attributed to the reduction of Cu^{II} with concomitant oxidation of the hfac ligands.³² However, these experiments were carried out at significantly higher substrate temperatures, 400 °C (compared to experiments reported here, 170 °C), where ligand decomposition might be expected.

Suppressing Impurities in the Cu Films Deposited in the Presence of Water. The incorporation of Cu₂O in the Cu films was suppressed by introducing hfach vapor during CVD. The hfach flow rate of 0.4 sccm was high enough to completely suppress the forward reaction in eqs 7–9. It was possible to reverse the reaction that forms Cu₂O because previous studies on dry-etching of copper oxides using hfach²⁸ and CVD involving Cu(hfac)₂ and H₂O in this study have shown that eq 7 is sufficiently close to equilibrium that it can proceed in either direction. The deposition rate and resistivity of the Cu films at low and high water vapor conditions were not affected by introduction of 0.4 sccm of hfach vapor and the films exhibited near bulk resistivities (~2.0 μΩ cm) with dense morphology. An XPS analysis showed that the films were pure Cu even under conditions of high water vapor when hfach was also introduced during CVD (Table 6).

Summary and Conclusions

The CVD of Cu using (hfac)CuL where L = VTMS or 2-butyne in the presence of water and other reagents has been studied to understand the deposition rate enhancement and impurity incorporation in the films. The overall CVD reaction in the presence of water is similar to the overall reaction in the absence of water. The data in this work support the idea that the rate-limiting reaction is the cleavage of the Cu–L bond on the surface. The presence of water can accelerate the dissociation of the L from the (hfac)CuL by hydrogen bonding with the hfac ligand and oxygen donation to the copper(I) center, resulting in the deposition rate enhancement. The presence of water during CVD also introduces a reaction pathway parallel to the main pathway for CVD of Cu. The parallel reaction is believed to occur via reaction of water with [Cu(hfac)] rather than liberated Cu(hfac)₂ and results in the incorporation of copper(I) oxide (Cu₂O) in the Cu films. The Cu films deposited at low water vapor flow rates (0.2 sccm) exhibited near bulk resistivities (~2.0 μΩ cm) and dense surface morphologies while the Cu films deposited at high water vapor flow rate (2.4 sccm) showed significantly higher resistivities (~12 μΩ cm) and porous morphologies. The incorporation of Cu₂O

was completely suppressed by introduction of hfacH vapor along with the precursor and water vapor during CVD of Cu. The introduction of small quantities of hfacH vapor did not affect the enhancement in deposition rate and allowed deposition of the high-purity copper necessary for IC metallization.

Acknowledgment. M.J.H.-S. and T.T.K. thank the NSF (CHE-9107035) and the Office of Naval Research (ONR) for funding this work. M.J.H.-S. thanks the NSF chemical instrumentation program for purchase of a low-field NMR spectrometer and ONR for analytical facilities. SIMS analyses were performed at the UNM/SNL Ion Microprobe Facility, a joint operation of the Institute of Meteoritics, University of New Mexico, and Sandia National Laboratories.

Supporting Information Available: X-ray crystallographic data for Cu(hfac)₂(H₂O), structure determination summary, atomic coordinates, bond lengths and angles, anisotropic displacement coefficients, and H-atom coordinates (13 pages); observed and calculated structure factor tables (6 pages). Ordering information is given on any current masthead page.

CM950546Y